Coupling Single Molecule Magnets to Ferromagnetic Substrates

A. Lodi Rizzini,[1] C. Krull,[1] T. Balashov,[1] J. J. Kavich,[1] A. Mugarza,[1] P. S. Miedema,[2] P. K. Thakur,[3] V. Sessi,[3] S. Klyatskaya,[4] M. Ruben,[4,5] S. Stepanow,[6] and P. Gambardella[1,7,8]

[1]*Catalan Institute of Nanotechnology (ICN-CIN2), UAB Campus, E-08193 Barcelona, Spain*
[2]*Debye Institute of Nanomaterials Science, Utrecht University, 3584 CA Utrecht, The Netherlands*
[3]*European Synchrotron Radiation Facility, BP 220, F-38043 Grenoble, France*
[4]*Institute of Nanotechnology, Karlsruhe Institute of Technology (KIT), D-76344 Eggenstein-Leopoldshafen, Germany*
[5]*Institute de Physique et Chimie de Matériaux de Strasbourg (IPCMS), UMR 7504, CNRS-Université de Strasbourg, F-67034 Strasbourg, France*
[6]*Max-Planck-Institut für Festkörperforschung, D-70569 Stuttgart, Germany*
[7]*Institució Catalana de Recerca i Estudis Avançats (ICREA), E-08100 Barcelona, Spain*
[8]*Departament de Física, Universitat Autònoma de Barcelona, E-08193 Barcelona, Spain*

(Received 12 May 2011; published 19 October 2011)

We investigate the interaction of $TbPc_2$ single molecule magnets (SMMs) with ferromagnetic Ni substrates. Using element-resolved x-ray magnetic circular dichroism, we show that $TbPc_2$ couples antiferromagnetically to Ni films through ligand-mediated superexchange. This coupling is strongly anisotropic and can be manipulated by doping the interface with electron acceptor or donor atoms. We observe that the relative orientation of the substrate and molecule anisotropy axes critically affects the SMM magnetic behavior. $TbPc_2$ complexes deposited on perpendicularly magnetized Ni films exhibit enhanced magnetic remanence compared to SMMs in the bulk. Contrary to paramagnetic molecules pinned to a ferromagnetic support layer, we find that $TbPc_2$ can be magnetized parallel or antiparallel to the substrate, opening the possibility to exploit SMMs in spin valve devices.

DOI: 10.1103/PhysRevLett.107.177205 PACS numbers: 75.50.Xx, 33.15.Kr, 75.30.Et, 75.70.−i

In future years the miniaturization of spintronic devices may require including molecular-scale elements in hybrid metal-organic architectures [1–4]. Single molecule magnets (SMMs) represent the smallest known bi-stable magnetic systems [5], thus making them ideal candidates for both classical and quantum computing applications [1,6]. Unfortunately, because of the competition between thermal spin fluctuations and magnetic anisotropy, SMMs display remanent magnetization only at low temperature. This occurs as magnetic relaxation becomes slow compared to the time scale of observations (τ), typically below 6 K in the archetypal Mn_{12} compound [5,7] and 40 K in mononuclear Tb double-decker complexes ($TbPc_2$) [8,9]. Measurements of $TbPc_2$, however, show that magnetic hysteresis is absent down to $T = 7$ K if τ is greater than about 100 s [10–13]. Increasing the magnetic stability of SMMs independently of temperature is thus one of the greatest challenges faced by molecular spintronics.

Efforts to slow down magnetic relaxation in SMMs have so far relied on the synthesis of polynuclear molecules with a large number of metal ions [14] or on modifying the ligand field strength in order to raise the magnetic anisotropy energy [15]. These approaches have been moderately successful. For example, ligand oxidation has been shown to increase the blocking temperature of $TbPc_2$ by about 10 K [16]. Recently, an alternative strategy has been proposed to stabilize the magnetic moment of paramagnetic molecules against thermal fluctuations, based on the deposition of metal-porphyrins and phthalocyanines on ferromagnetic (FM) films [17–23]. Because of the planar structure of such molecules and close proximity of the metal ions to the substrate, the magnetic moment of the metal centers can efficiently couple to the surface magnetization via superexchange and direct exchange paths [19–22]. Although individual molecules cannot be magnetized independently, this approach enables the fabrication of metal-organic layers with stable magnetization up to room temperature [18,20,23]. Ultrathin molecular layers may thus be used to fabricate FM heterostructures or magnetochemical sensors [23].

In this Letter, we investigate the coupling between SMMs and FM substrates. We focus on $TbPc_2$ owing to its compact structure, which constitutes an advantage to establish an exchange path between the magnetic core of the molecule and the ferromagnet. We choose Ni layers for the substrate, as the direction of the easy axis can be controlled through epitaxial strain without changing the chemical composition of the SMM/FM interface. Using x-ray magnetic circular dichroism (XMCD), we show that $TbPc_2$ SMMs couple antiferromagnetically (AFM) to a FM metal. We determine the magnitude of the exchange coupling constants and show how these can be enhanced (reduced) by increasing (decreasing) the amount of charge transferred from the surface to the molecules. Our results evidence the competition between the SMM and substrate magnetic anisotropy, and show that the magnetic moment of $TbPc_2$ can be effectively stabilized against thermal fluctuations while preserving typical SMM features.

The experiments were performed at beam line ID08 of the European Synchrotron Radiation Facility (ESRF). The samples were prepared *in situ* by molecular beam evaporation of $TbPc_2$ on Ni films in ultrahigh vacuum. The $TbPc_2$ coverage was 0.05 ± 0.02 monolayers (ML). FM films with out-of-plane (OP) and in-plane (IP) magnetic anisotropy were obtained by deposition of 13 ML of Ni on Cu(100) and 6 ML of Ni on Ag(100) sputter-annealed single crystals, respectively [24,25]. Oxidized and reduced Ni surfaces with OP magnetization were prepared by the surfactant growth of a $c(2 \times 2)$ O phase on Ni/Cu(100) [26] and by evaporating Li on $TbPc_2$/Ni/Cu(100). $TbPc_2$ adsorbs flat on metal surfaces [10,27] as well as on oxygen-covered Ni [28]. The XMCD measurements were carried out using total electron yield detection at the $L_{2,3}$ absorption edges of Ni and $M_{4,5}$ absorption edges of Tb, selectively probing the substrate ($\mathbf{M}_{\mathrm{Ni}}$) and molecule ($\mathbf{M}_{\mathrm{Tb}}$) magnetic moments. A magnetic field $\mathbf{B}$ was applied parallel to the x-ray direction at normal ($\theta = 0°$) and grazing ($\theta = 70°$) incidence to measure the OP and IP magnetization. The time required to record a set of Tb XMCD spectra or a hysteresis loop was about 10^3 s, which defines the lower limit of τ probed in this experiment. For more details about the beam line setup, sample preparation, and XMCD measurements we refer to Refs. [10,30].

We begin by investigating the coupling of $TbPc_2$ to OP Ni films, in which case the molecule and substrate easy axes are collinear. Figure 1(a) shows the Ni and Tb x-ray absorption (XAS) and XMCD spectra recorded at $T = 8$ K after saturating the magnetization at 5 T and subsequently setting the field to zero. We observe that both Ni and Tb have a strong remanent XMCD intensity, which remains stable over the time scale of the measurements. The sign of the Tb XMCD, however, is opposite to Ni, indicating that $\mathbf{M}_{\mathrm{Tb}}$ and $\mathbf{M}_{\mathrm{Ni}}$ are AFM coupled. Measurements of $TbPc_2$ on IP Ni films, reported in Fig. 1(b), illustrate the case where the molecule and substrate easy axes are orthogonal. Although the coupling between $TbPc_2$ and Ni remains antiferromagnetic, as expected, the remanent Tb XMCD intensity along the substrate easy axis is now strongly reduced compared to the Ni XMCD. This result shows the importance of matching the substrate and SMM magnetic anisotropy properties to effectively stabilize the SMM magnetization in the absence of external magnetic fields. Notably, this is in contrast with recent theoretical calculations of Mn_{12} on Ni, which postulate that the magnetic easy axis of the SMM-substrate system is dictated by that of the Ni layer [31].

Element-resolved hysteresis loops provide further insight into the nature of SMM-substrate coupling. Figure 2(a) shows the out-of-plane ($\theta = 0°$) and in-plane ($\theta = 70°$) magnetization loops of the OP $TbPc_2$/Ni/Cu(100) sample measured by recording the XMCD intensity at the Ni L_3 and Tb M_5 edge as a function of applied field [28]. In the low field region, $\mathbf{M}_{\mathrm{Tb}}$ is aligned

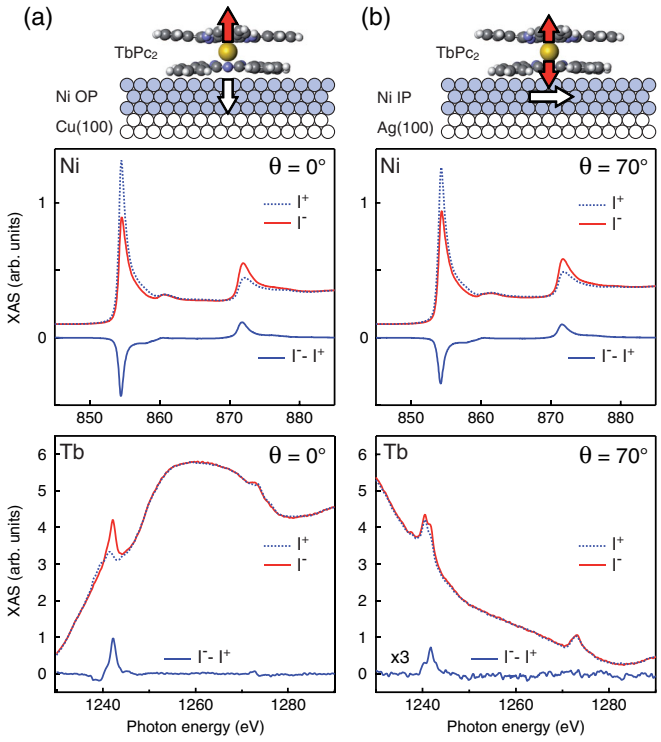

FIG. 1 (color online). XMCD measurements of $TbPc_2$ on (a) OP Ni/Cu(100) and (b) IP Ni/Ag(100) films recorded at remanence, $T = 8$ K. Top: schematic view of the $TbPc_2$ and Ni magnetization. Middle: XAS spectra measured at the $L_{2,3}$ edges of Ni with positive (I^+) and negative (I^-) circular polarization, and XMCD intensity ($I^- - I^+$). Bottom: Tb spectra at the $M_{4,5}$ edges. Because of the low $TbPc_2$ coverage, the Tb XAS is superimposed to a substrate-dependent background.

antiparallel to $\mathbf{M}_{\mathrm{Ni}}$, switching direction together with it [dashed lines in Fig. 2(a)]. Note that $\mathbf{M}_{\mathrm{Tb}}$ does not present a butterfly hysteresis loop with near-zero remanence typical of $TbPc_2$ in bulk crystals and nonmagnetic substrates [11,13,32], but closely follows the square $\mathbf{M}_{\mathrm{Ni}}$ loop as long as $B < 0.1$ T. At higher field, however, the Zeeman interaction overcomes antiferromagnetic exchange, inducing a gradual rotation of $\mathbf{M}_{\mathrm{Tb}}$ parallel to $\mathbf{B}$. $\mathbf{M}_{\mathrm{Tb}}$ first changes sign at $B = B_{\mathrm{exc}}$, as the external field compensates the exchange coupling to the substrate, and finally ends up parallel to $\mathbf{M}_{\mathrm{Ni}}$. A similar behavior is observed for the out-of-plane (left panel) and in-plane $\mathbf{M}_{\mathrm{Tb}}$ (right panel), albeit the Tb remanence, B_{exc}, and the magnetization at high-field depend on the orientation of $\mathbf{B}$ with respect to the SMM easy axis.

The coupling between $\mathbf{M}_{\mathrm{Tb}}$ and $\mathbf{M}_{\mathrm{Ni}}$ is necessarily mediated by the bottom Pc ligand of $TbPc_2$, which separates the Tb ion from the surface. This likely occurs through electrons residing or transferred into a Pc π orbital. Therefore, we tested the possibility of tuning the exchange interaction by modifying the amount of charge transfer between surface and molecule. This can be realized in practice by (i) preparing a (2×2) O buffer layer

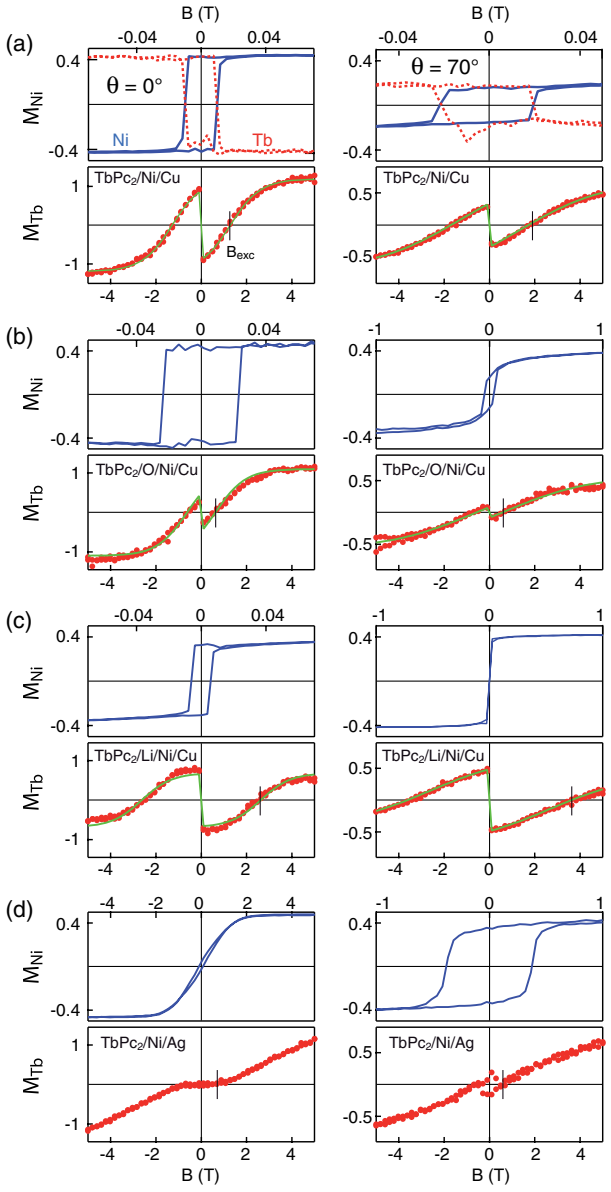

FIG. 2 (color online). Element-resolved hysteresis loops of Ni (top) and Tb (bottom) for (a) $TbPc_2$/Ni/Cu(100), (b) $TbPc_2$/O/Ni/Cu(100), (c) $TbPc_2$/Li/Ni/Cu(100), and (d) $TbPc_2$/Ni/Ag(100) measured at normal (left) and grazing (right) incidence at $T = 8$ K. The units of $\mathbf{M}_{Ni}$ and $\mathbf{M}_{Tb}$ correspond to the XMCD/XAS ratio at the L_3 and M_5 absorption edges, respectively [28]. The dashed lines in (a) show the Tb magnetization at low field normalized to $\mathbf{M}_{Ni}$. The solid lines superposed to $\mathbf{M}_{Tb}$ are fits according to Eq. (1).

[26] between $TbPc_2$ and Ni, and (ii) "doping" the Ni surface with a strong electron donor such as Li. Although we do not control the extent of charge transfer in either case, it is safe to assume that (i) leads to oxidation and (ii) to a reduction of the Pc ligand. The reproducibility of the XMCD spectral features proves that the electronic configuration of Tb remains predominantly $4f^8$ in either case [28,29]. However, we observe a reduction of the XMCD/XAS ratio for $TbPc_2$/Li/Ni/Cu(100) [28], which is consistent with moderate charge transfer into the $4f$ states, as would be expected due to increased occupancy of the Pc orbitals [12]. The effects of charge transfer on the Ni magnetization, reported in Figs. 2(b) and 2(c), are limited to changes of the coercivity, which we ascribe to modifications of the surface magnetocrystalline anisotropy energy. The magnetic behavior of $TbPc_2$, on the other hand, changes significantly. The remanent $\mathbf{M}_{Tb}$ decreases strongly in $TbPc_2$/O/Ni layers compared to $TbPc_2$/Ni, as shown in Fig. 2(b). Moreover, B_{exc} varies from 0.6 T in $TbPc_2$/O/Ni to 2.5 T in $TbPc_2$/Li/Ni [Fig. 3(a)], indicating that the exchange coupling energy increases significantly with the amount of charge donated to the Pc ligand.

The competition between the intrinsic SMM properties, namely, the magnetic anisotropy, Zeeman interaction of $TbPc_2$, and antiferromagnetic exchange to the substrate, can be described using the following Hamiltonian:

$$H = \mu_B(\mathbf{L} + 2\mathbf{S}) \cdot \mathbf{B} - \lambda \mathbf{L} \cdot \mathbf{S} + V_{CF} + \hat{\mathbf{M}}_{Ni} \cdot \mathbf{K} \cdot \hat{\mathbf{S}} \quad (1)$$

where μ_B is the Bohr magneton, $\mathbf{S}$ and $\mathbf{L}$ the spin and orbital moments of Tb, $\lambda = 212$ meV the spin-orbit energy, and $V_{CF} = -B_2O_2^0 - B_4O_4^0 - B_6O_6^0$ the Tb crystal field potential as a function of the Stevens operators O_k^m. Since V_{CF} is not affected by deposition on metals [10], we use the same coefficients $B_2 = 414$, $B_4 = -228$, and $B_6 = 33$ cm^{-1} as for the free molecule, which give a magnetic anisotropy barrier of about 590 cm^{-1} (73 meV) [9,33]. $\mathbf{K}$ represents the superexchange tensor between Ni and Tb, of which we consider only the diagonal out-of-plane $K^{\perp}$ and in-plane $K^{\parallel}$ components. The dipolar magnetic field produced by the substrate can be neglected [28]. We use Eq. (1) to calculate the expectation value of $\mathbf{M}_{Tb} = -\mu_B(\langle \mathbf{L} \rangle + 2\langle \mathbf{S} \rangle)$ as a function of applied field and temperature and fit the curves reported in Fig. 2. The fit is restricted to the bottom $J = L + S = 6$ multiplet of $TbPc_2$ [33]. For simplicity, we take $\hat{M}_{Ni} = \pm 1$ for $B \gtrless 0$. The fit has three free parameters: $K^{\perp}$, $K^{\parallel}$, and a multiplicative

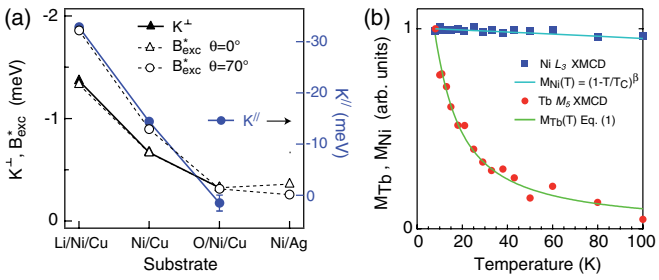

FIG. 3 (color online). (a) Exchange field (B_{exc}) and coupling constants ($K^{\perp}$, $K^{\parallel}$) derived from Fig. 2 and Eq. (1), respectively. (b) Temperature dependence of the remanent Ni and Tb XMCD intensity, normalized to the values at $T = 8$ K. Solid lines represent the calculated $\mathbf{M}_{Tb}$ and $\mathbf{M}_{Ni}$ (see text).

factor that scales $\mathbf{M}_{\mathrm{Tb}}$ to the XMCD intensity. Such parameters reduce to two when $\theta = 0°$ for the curves shown in Figs. 2(a)–2(c), where $K^{\parallel}$ plays no role. The results, shown as solid lines, reproduce remarkably well the easy and hard axis behavior of $TbPc_2$, demonstrating that our model captures the main features of the interaction between SMM and OP substrates. The situation appears to be more complicated for the IP substrate [Fig. 2(d)], where $\mathbf{M}_{\mathrm{Tb}}$ saturates at a slower rate compared to the OP case. Presently, we cannot explain such a difference using Eq. (1). However, we can qualitatively interpret the shape of the out-of-plane loop [left panel in Fig. 2(d)], where $\mathbf{M}_{\mathrm{Tb}}$ is approximately zero up to $B = \pm 0.7$ T. This peculiar behavior is consistent with the fact that, due to the strong perpendicular anisotropy, only the out-of-plane component of $\mathbf{M}_{\mathrm{Ni}}$ can polarize $\mathbf{M}_{\mathrm{Tb}}$, whereas the in-plane exchange field mixes in equal amount up and down magnetic states. As long as M_{Ni} is linear with B, the out-of-plane antiferromagnetic exchange term $K^{\perp}\hat{M}_{\mathrm{Ni}}$ compensates the Zeeman energy $\mu_B(\mathbf{L} + 2\mathbf{S})B$, leading to $M_{\mathrm{Tb}} \approx 0$.

Figure 3(a) compares the values of $K^{\perp}$, $K^{\parallel}$, and $B^{*}_{\mathrm{exc}} = \mu_B(L + 2S)B_{\mathrm{exc}}$ measured at $\theta = 0°$ and 70°. We observe that $K^{\perp}$ and $B^{*}_{\mathrm{exc}}(\theta = 0°)$ nearly match each other, as expected for an Ising-like system. $K^{\perp}$ increases by about a factor of 4 going from $TbPc_2$/O/Ni to $TbPc_2$/Li/Ni. Moreover, we find that $\mathbf{K}$ is strongly anisotropic, since $K^{\parallel}$ is generally much greater than $K^{\perp}$. Such a strong superexchange anisotropy is not unusual for rare earth ions with unquenched $\mathbf{L}$ since the spin-orbit interaction is significant compared to V_{CF} [34]. In such a case, a rotation of the $4f$ spin carries the orbital wave functions with it, thereby significantly varying the electronic overlap with neighboring orbitals that is at the origin of superexchange.

Finally, we address the magnetic stability of $TbPc_2$ on Ni as a function of temperature. From the data reported in Fig. 2, it is evident that the interaction with Ni greatly enhances $\mathbf{M}_{\mathrm{Tb}}$ at zero field compared to $TbPc_2$ in the bulk and on nonmagnetic substrates [11,13], where resonant quantum tunnelling between hyperfine levels prevents reaching 100% remanence [32]. Figure 3(b) shows that finite remanence is observed up to $T = 100$ K, indicating that the coupling with Ni stabilizes $\mathbf{M}_{\mathrm{Tb}}$ on a time scale of the order of 10^3 s. The solid lines represent $M_{\mathrm{Tb}}(T)$ calculated using Eq. (1) and $M_{\mathrm{Ni}}(T) = (1 - T/T_C)^{\beta}$, with $T_C = 575$ K and $\beta = 0.28 \pm 0.04$ [24]. Note that $\mathbf{M}_{\mathrm{Tb}}$ relaxes independently of $\mathbf{M}_{\mathrm{Ni}}$, as expected for a paramagnetic system described by Eq. (1) in the presence of an exchange field.

Before concluding, we provide a comparison of our results with previous measurements of paramagnetic molecules deposited on FM metal films [18–23]. Unlike the above systems, the magnetic metal ion of $TbPc_2$ is separated from the surface by a complex ligand structure and has f rather than d character. The coupling of $TbPc_2$ to Ni is antiferromangetic, whereas metal-porphyrins and phthalocyanines always couple ferromagentically to bare metal surfaces either through direct exchange or by 90° superexchange [17–23]. Both mechanisms are unlikely to occur in SMMs because the metal centers are placed further away from the surface. Such separation also favors 180° antiferromangetic superexchange paths over 90° FM ones. Most importantly, the magnetization of metal-porphyrins and phthalocyanines always mimic that of the FM substrate, whereas $TbPc_2$ and Ni clearly behave as two different magnetic systems. This is attributed to the smaller superexchange interaction of SMMs compared to planar molecules [20] as well as to the strong magnetic anisotropy and large magnetic moment intrinsic to SMMs.

In summary, we have proven that SMMs couple to FM metal layers. The superexchange interaction mediating the coupling can be tuned by oxidizing or reducing the FM substrate. Element-resolved hysteresis curves reveal that the SMM magnetization depends critically on the alignment of the molecule and substrate easy axes as well as on the balance between interface-dependent superexchange and applied magnetic field. All together, our results show that SMMs behave as coupled but separate magnetic units from an underlying FM surface. The enhanced thermal stability of the $TbPc_2$ magnetic moment and the possibility to orient it parallel or antiparallel to a macroscopic FM layer make $TbPc_2$ very interesting for applications in hybrid devices. Future experiments may address the coupling of different SMM families to ferromagnets as well as the transport properties of SMM-FM spin valves.

We acknowledge support from the European Research Council (StG 203239 NOMAD), Ministerio de Ciencia e Innovación (MAT2010-15659), and Agència de Gestió d'Ajuts Universitaris i de Recerca (2009 SGR 695). A. M. acknowledges funding from the Ramon y Cajal Fellowship program.

[1] L. Bogani and W. Wernsdorfer, Nature Mater. **7**, 179 (2008).
[2] P. Gambardella *et al.*, Nature Mater. **8**, 189 (2009).
[3] M. Mannini *et al.*, Nature Mater. **8**, 194 (2009).
[4] A. Mugarza *et al.*, Nature Commun. **2**, 490 (2011).
[5] R. Sessoli, D. Gatteschi, A. Caneschi, and M. A. Novak, Nature (London) **365**, 141 (1993).
[6] M. N. Leuenberger and D. Loss, Nature (London) **410**, 789 (2001).
[7] A. Fort *et al.*, Phys. Rev. Lett. **80**, 612 (1998).
[8] N. Ishikawa *et al.*, J. Am. Chem. Soc. **125**, 8694 (2003).
[9] F. Branzoli *et al.*, J. Am. Chem. Soc. **131**, 4387 (2009).
[10] S. Stepanow *et al.*, J. Am. Chem. Soc. **132**, 11 900 (2010).
[11] L. Margheriti *et al.*, Adv. Mater. **22**, 5488 (2010).
[12] R. Biagi *et al.*, Phys. Rev. B **82**, 224406 (2010).
[13] M. Gonidec *et al.*, J. Am. Chem. Soc. **133**, 6603 (2011).
[14] P.-H. Lin *et al.*, Angew. Chem. **121**, 9653 (2009).

[15] S. Takamatsu *et al.*, Inorg. Chem. **46**, 7250 (2007).
[16] N. Ishikawa *et al.*, Inorg. Chem. **43**, 5498 (2004).
[17] T. Suzuki, M. Kurahashi, and Y. Yamauchi, J. Phys. Chem. B **106**, 7643 (2002).
[18] A. Scheybal *et al.*, Chem. Phys. Lett. **411**, 214 (2005).
[19] H. Wende *et al.*, Nature Mater. **6**, 516 (2007).
[20] M. Bernien *et al.*, Phys. Rev. Lett. **102**, 047202 (2009).
[21] C. Iacovita *et al.*, Phys. Rev. Lett. **101**, 116602 (2008).
[22] S. Javaid *et al.*, Phys. Rev. Lett. **105**, 077201 (2010).
[23] C. Wäckerlin *et al.*, Nature Commun. **1**, 61 (2010).
[24] F. Huang, M. T. Kief, G. J. Mankey, and R. F. Willis, Phys. Rev. B **49**, 3962 (1994).
[25] B. Schulz and K. Baberschke, Phys. Rev. B **50**, 13467 (1994).
[26] R. Nünthel *et al.*, Surf. Sci. **531**, 53 (2003).
[27] L. Vitali *et al.*, Nano Lett. **8**, 3364 (2008).
[28] See Supplemental Material at http://link.aps.org/supplemental/10.1103/PhysRevLett.107.177205 for information on the orientation of $TbPc_2$ molecules, magnetization curves measured by XMCD, changes of the XMCD line shape induced by O and Li doping, and dipolar field induced by the FM substrate.
[29] B. T. Thole, G. van der Laan, J. C. Fuggle, G. A. Sawatzky, R. C. Karnatak, and J.-M. Esteva, Phys. Rev. B **32**, 5107 (1985).
[30] S. Stepanow *et al.*, Phys. Rev. B **82**, 014405 (2010).
[31] K. Park, Phys. Rev. B **83**, 064423 (2011).
[32] N. Ishikawa, M. Sugita, and W. Wernsdorfer, Angew. Chem., Int. Ed. **44**, 2931 (2005).
[33] N. Ishikawa *et al.*, Inorg. Chem. **42**, 2440 (2003).
[34] J. M. Baker, Rep. Prog. Phys. **34**, 109 (1971).